Journal of Solid State Chemistry 182 (2009) 2591–2597

Contents lists available at ScienceDirect

Journal of Solid State Chemistry

journal homepage: www.elsevier.com/locate/jssc

Synthesis and characterization of nanometric powders of UO_{2+x}, $(Th,U)O_{2+x}$ and $(La,U)O_{2+x}$

G. Rousseau [a,b,c,d], M. Fattahi [a], B. Grambow [a], L. Desgranges [b], F. Boucher [c], G. Ouvrard [c], N. Millot [d,*], J.C. Nièpce [d]

[a] Ecole des Mines de Nantes, SUBATECH, UMR 6457, 4, rue Alfred Kastler, BP 20722, 44307 Nantes, France
[b] CEA Cadarache, DEN/DEC/SA3C/L2EC, Bât. 315, 13108 Saint-Paul-les-Durance, France
[c] Institut des Matériaux Jean Rouxel, UMR 6502, 2, rue de la Houssinière, BP 32229, 44322 Nantes, France
[d] Institut Carnot de Bourgogne, UMR 5209 CNRS/Université de Bourgogne, 9 Avenue Alain Savary, BP 47870, 21078 Dijon cedex, France

ARTICLE INFO

Article history:
Received 24 March 2009
Received in revised form
23 June 2009
Accepted 24 June 2009
Available online 30 June 2009

Keywords:
Precipitation
Electrochemical reduction
Nanometric particles
UO_2
Powders characterization

ABSTRACT

This paper describes a new way of preparing nanometric powders of uranium oxide, to fit the needs of studies on UO_2 oxidation, through the electrochemical reduction of U(VI) into U(IV). These powders can also be doped with radionuclides if necessary. The precipitation of oxides occurs in reducing and anoxic conditions. This original method makes it possible to synthesize nanometric UO_2 powders with a calibrated size, as well as the Th- and La-doped UO_2 powders with a predefined composition. The powder characterization by the X-ray diffraction, X-ray photoelectron spectroscopy and transmission electron Microscopy shows the formation of spherical crystallites of UO_{2+x}, $(Th,U)O_{2+x}$ and $(La,U)O_{2+x}$ phases. The composition can be defined by the initial Th/(Th+U) and La/(La+U) ratios in solution and the particle size can be controlled by varying the pH.

1. Introduction

The oxidation of uranium dioxide has been studied for more than 50 years. It was first studied [1 and references therein] for fuel fabrication purposes and then later on for safety purposes to design a dry storage facility for spent nuclear fuel that could last several hundred years [2]. Therefore, knowledge of the changes occurring during the oxidation process is essential and a sound prediction of the behavior of uranium oxides requires an accurate description of the elementary mechanisms occurring on an atomic scale. Only the models based on elementary mechanisms should be able to provide a reliable extrapolation of laboratory results over timeframes spanning several centuries. The oxidation of UO_2 powders is usually partitioned in two stages: the first is associated with a pseudo-parabolic weight gain curve, while the second is associated with a sigmoid weight gain curve [3]. The pseudo-parabolic curve, attributed the formation of U_4O_9 and U_3O_7 on UO_2 powders, indicates a diffusion-controlled mechanism [4]. This mechanism was modeled with a finite difference algorithm [5] that was recently developed. The sigmoid curve is generally interpreted as the oxidation of U_3O_7 into U_3O_8 with a nucleation and growth mechanism [6]. This sigmoid curve is still a subject of debate in its quantitative interpretation. More precisely, the apparent activation energy for U_3O_8 formation deduced from the kinetic analysis of the experimental sigmoid curves, based on Avrami type laws, differs widely from 48 to 194 $kJ\,mol^{-1}$ depending on the authors [6]. It was recently proven [7] that macro-cracking of the initial UO_2 sample changes the weight gain curves from which the apparent activation energy is deduced. Therefore, the actual activation energy of U_3O_8 can only be obtained on a sample unaffected by macro-cracking, i.e., powders with a grain size less than the critical size needed for macro-cracking [7–9]. The available industrial powders, obtained in dry or wet conditions, have an inhomogeneous grain size and are agglomerated. Moreover, some grains are stuck together and can be separated using oxidation by macro-cracking, which makes them unexploitable for a study on the U_3O_8 activation energy. Some UO_2 nanoparticles were recently produced by irradiating U(VI) solutions with electrons and γ-radiation [10], which yielded small particles with a narrow size distribution (22–35 nm). However, the powder did not consist of stoichiometric UO_2, but rather of a mixture of oxidation states: U(IV), U(V) and U(VI), with the likely existence of hydroxide or oxo-hydroxide phases, making them unusable for a proper study on UO_2 oxidation.

This paper describes an original method that can be used to synthesize UO_2 powders by the wet process, and thus avoid the drawbacks associated with industrial powders. The method is

---

* Corresponding author.
E-mail address:
nmillot@u-bourgogne.fr (N. Millot).

0022-4596/$ - see front matter © 2009 Elsevier Inc. All rights reserved.
doi:10.1016/j.jssc.2009.06.039

based on the electrochemical reduction of U(VI) into U(IV) and the precipitation of UO_2 in reducing and anoxic conditions at a constant pH. Moreover, the behavior of irradiated UO_2 depends on its radionuclide content, which means it is necessary to have radionuclide-doped UO_2 powders to reproduce the behavior of irradiated fuel. It will be shown that this technique can also be used to obtain UO_2 powders with different grain sizes and doped with tetravalent or trivalent elements [11,12].

2. Experimental

2.1. Starting solutions

All solutions were prepared with degassed Milli-Q water (Millipore, 18 MΩ cm) and all chemicals used were of analytical purity. Stock solutions of U(VI), Th(IV) and La(III) were, respectively, prepared by dissolving $UO_2(NO_3)_2 \cdot 6H_2O$, $Th(NO_3)_4 \cdot 4H_2O$ and $La(NO_3)_3 \cdot 6H_2O$ in 1 M NaCl. Different starting solutions with different Th/(Th+U) and La/(La+U) ratios were prepared from these stock solutions. The HCl and NaOH stock solutions were prepared in a glove box (MBraun, MB-200 with an extension model MB-200 MOD-E 1250/1000) under a nitrogen atmosphere, using the degassed water. The U(IV) stock solution was prepared in the glove box by electrolytic reduction of the initial U(VI) nitrate solution in the absence of O_2. The pH of this solution was kept below 1 to ensure the stability of U(IV). The U(IV) absorption spectrum was monitored periodically by a UV–vis spectrophotometer (Shimadzu, UV-2401PC) connected directly to the glove box by optical glass fibers (from 350 to 750 nm) capable of indicating a decrease in the U(IV) concentration with a sensitivity of 1%.

2.2. Synthesis method

All experiments were performed in a glove box under a nitrogen atmosphere for several days inside a reaction vessel containing 1 M NaCl (50–100 mL) at ambient temperature. The method is based on the electrochemical reduction of U(VI) into U(IV) using a galvanostat (Radiometer Voltalab 21), with the precipitation of UO_2, doped or not, occurring in reducing and anoxic conditions (N_2 bubbling) at a constant pH. Two synthesis methods were possible depending on the pH.

In the pH-range of 2.5–4, only UO_{2+x} and $(Th,U)O_{2+x}$ were studied. In fact, a previous publication showed that the precipitation of La(III) with UO_{2+x} only occurred for pH higher than 6 [13]. Therefore, an aliquot of the starting U(VI) or (U(VI)+Th) solutions were added to the NaCl solution under reducing conditions (Fig. 1). U(VI) was reduced electrochemically to U(IV) at a fixed pH and UO_{2+x} or $(Th,U)O_{2+x}$ precipitated. The pH increases due to the coulometric titration as compensated by the continuous addition of necessary quantities of the titration solution (HCl 0.1 M).

In the pH-range of 4–8, this method of synthesis did not lead directly to the precipitation of U(IV) solid phases, but first to the formation of schoepite or Na-polyuranates due to the high initial uranium concentration (0.005 m). Then the reductive dissolution of the U(VI) phases was too slow to allow for the formation of UO_2. In order to avoid U(VI) precipitation, the dissolved U(IV), or (U(IV)+Th(IV)), or (U(IV)+La(III) (0.03 M, $pH < 1$)) was, therefore, added slowly using an automatic burette (Titrino 718 STAT Metrohm), directly to the 1 M NaCl solution at the selected pH value (Fig. 2). The addition of this solution acidified the solution, which was counterbalanced by adding NaOH (0.1 mol/L) to keep the pH constant.

The stability of the reducing conditions in starting solutions, during both the test and sampling, was insured by various methods. Fig. 3 presents the solubility diagram of UO_2^{2+}/U^{4+} at 25 °C as a function of redox potential ($-5 < pe < 10$) for pH between 4.5 and 10 [14]. The redox potential, *pe*, is calculated from the measured potential, Eh, versus the normal hydrogen electrode (NHE) according to the following equation:

$$pe = \frac{E_h(\mathrm{mV})}{59.2}$$

The solid phases controlling the solubility are also indicated. Based on this figure, it is necessary to ensure a reduction potential lower than −150 mV/NHE ($pe = -2.5$) in the pH-range of 5 to 9 to remain in the stability range of $UO_{2(cr)}$. This is indicated by the dotted line (Fig. 3). Hence, the redox potential Eh was fixed at −300 mV/N.H.E. In the pH-range of 2.5–4, the reduction potential was obtained by the UO_2^{2+}/U^{4+} equilibrium, making it possible to remain in the stability range of water.

Hence, all tests were run under permanent coulometric reduction conditions, which were ensured by two platinum electrodes (Radiometer Analytical). These electrodes were specially engineered for our experiment [11]. Because U(IV) readily oxidizes into U(VI) in the presence of O_2 both during the experiment and sampling, the removal of the oxygen traces of about 0.1 ppm in nitrogen gas was ensured using a redox cycle [11,15]. The nitrogen gas, containing oxygen traces (<100 ppb) was splashed through a NH_4VO_3 solution containing a ZnHg amalgam. The vanadium solution was used as a color indicator. When the amalgam was no longer efficient, the violet vanadium (II) was oxidized by oxygen to form red–brown peroxovanadium cation. The purified nitrogen gas was then saturated with Milli-Q

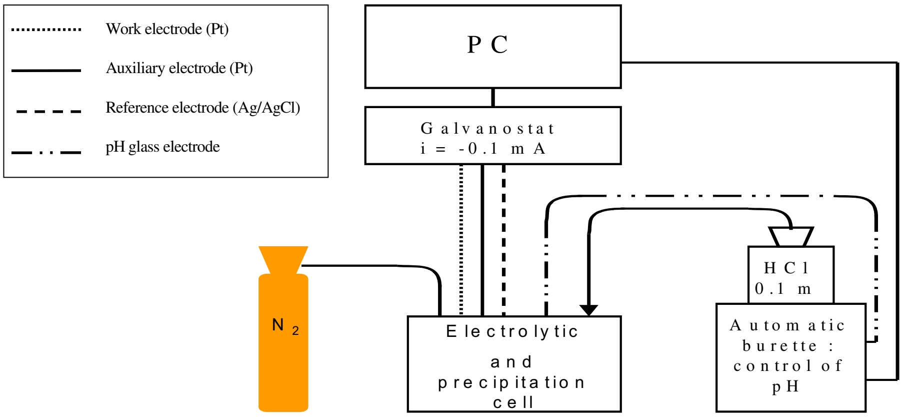

Fig. 1. Schematic diagram of the first synthesis method: UO_{2+x} and $(Th, U)O_{2+x}$ nanopowders obtained in the pH-range of 2.5–4.